Electronic Supplementary Material (ESI) for Physical Chemistry Chemical Physics.

Impact of charge state on 193 nm ultraviolet photodissociation of protein complexes

Sarah N. Sipe and Jennifer S. Brodbelt
Department of Chemistry
University of Texas at Austin
Austin, TX 78712

jbrodbelt@cm.utexas.edu

Supporting Information

Table S1. Range of charge states obtained from each of the solutions for each of the protein complexes. Charge states with insufficient abundances for MS/MS analysis are not included. The full range of charge states observed are shown in Figures 1 and S1-S4.

Protein Complex	MW / oligomeric state	Charge state distribution[1]		
		Supercharging	Standard	Charge-reducing
Cu/Zn Superoxide dismutase	31 kDa/ homodimer	- - -	10+ - 11+	8+ - 9+
Streptavidin	52 kDa / homotetramer	15+	13+ - 14+	10+ - 11+
Transthyretin	56 kDa/ homotetramer	16+ - 17+	13+ - 15+	11+ - 12+
Hemoglobin	64 kDa/ heterotetramer	- - -	15+ - 17+	11+ - 13+
C-reactive protein	115 kDa/ homopentamer	26+ - 27+	23+ - 25+	17+ - 19+

[1] The solution conditions are as follows: 20 mM m-NBA and 80 mM ammonium acetate for supercharging conditions; 100 mM ammonium acetate for standard native conditions, and 20 mM TEAA and 80 mM ammonium acetate for charge-reducing conditions.

Table S2. Structural features of each protein complex as observed from the associated PDB structures. Average interfacial area and number of hydrogen bonds (HB) and salt bridges (SB) for each subunit were obtained from PDBePISA. Values for Hb were averaged for α and β subunits.

Complex	Subunits	PDB	Disulfide Bonds	Interfacial contacts		
				Area (Å^2)	HB	SB
SOD	2	1CB4	1	661	5	0
SA	4	1SWB	0	2139	25	3
TTR	4	4TLT	0	1620	31	1
Hb	4	1BBB	0	1578	16	2
CRP	5	1B09	1	1275	14	16

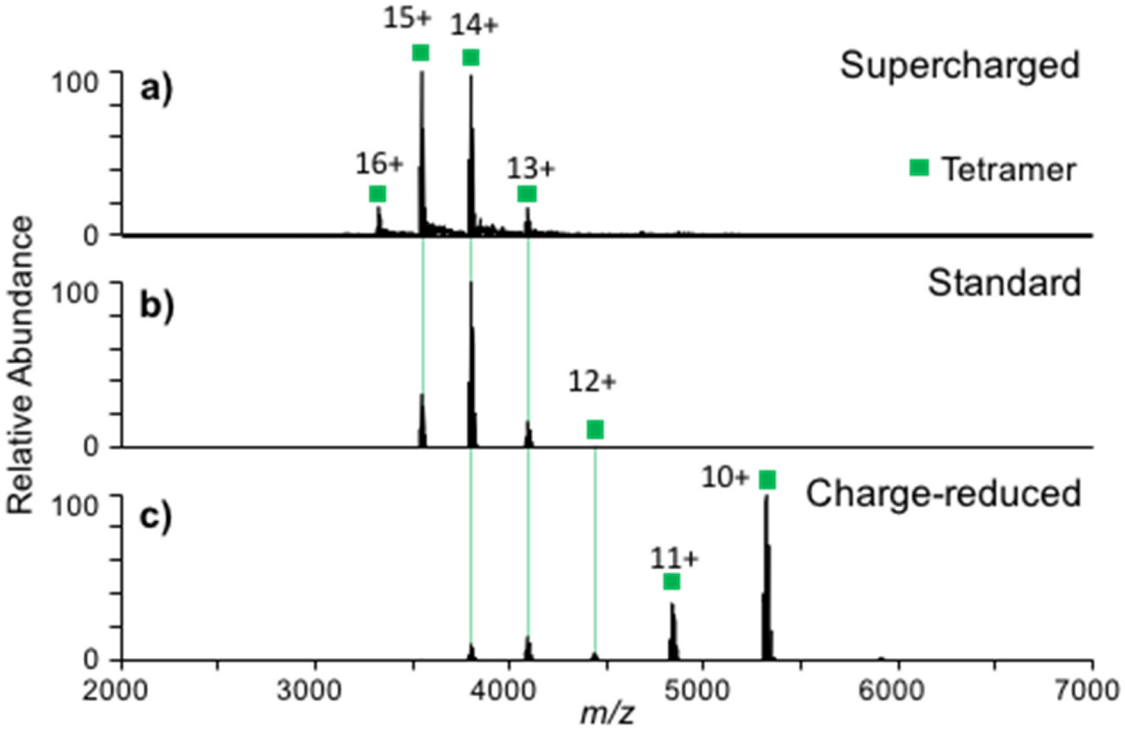

Figure S1. ESI-MS of streptavidin in a) 20 mM m-NBA, 80 mM ammonium acetate solution for supercharging, b) 100 mM ammonium acetate (standard native MS solution), and c) 20 mM triethylammonium acetate, 80 mM ammonium acetate for charge-reducing native solutions.

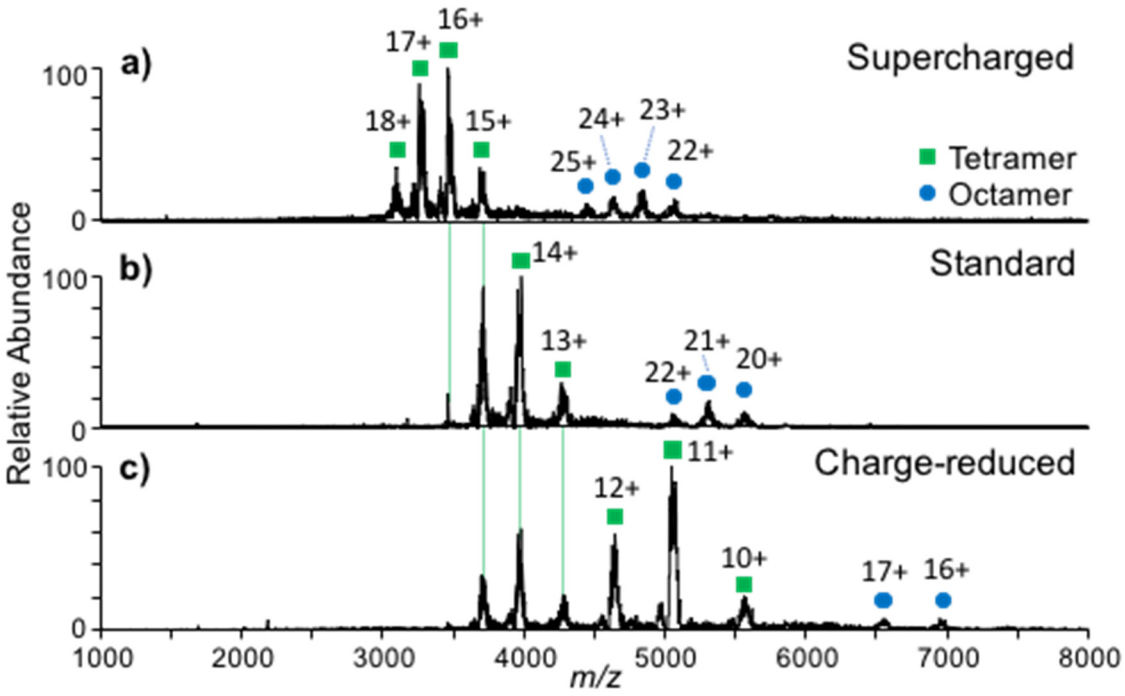

Figure S2. ESI-MS of transthyretin in a) 20 mM m-NBA, 80 mM ammonium acetate solution for supercharging, b) 100 mM ammonium acetate (standard native MS solution), and c) 20 mM triethylammonium acetate, 80 mM ammonium acetate for charge-reducing native solutions.

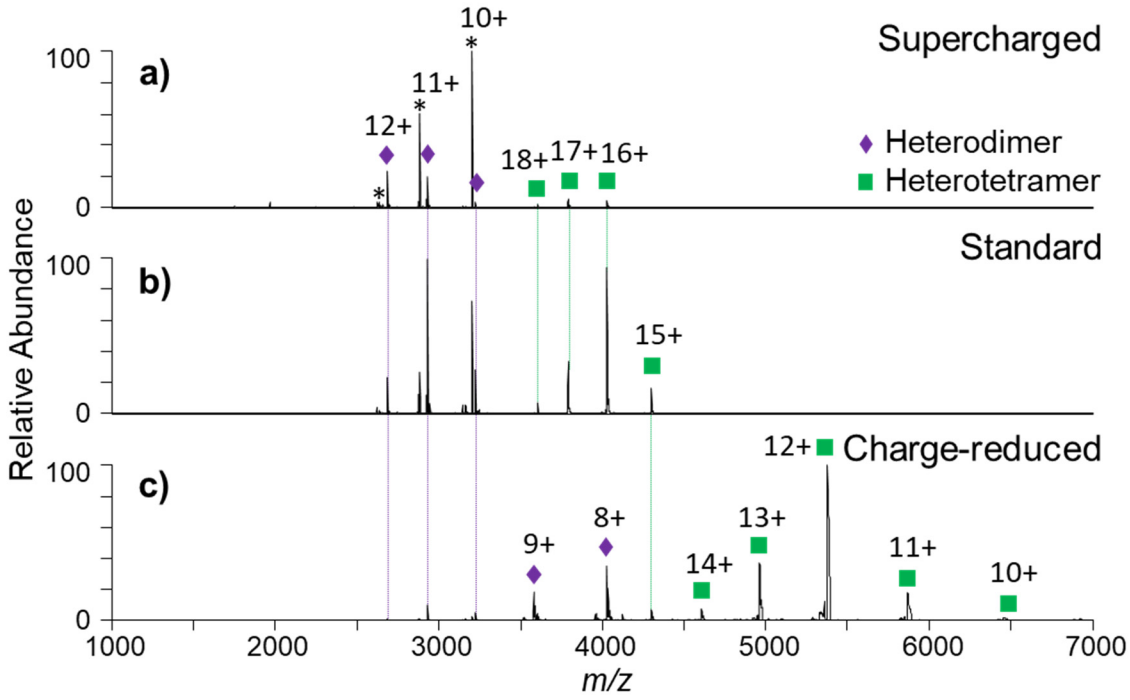

Figure S3. ESI-MS of hemoglobin in a) 20 mM m-NBA, 80 mM ammonium acetate solution for supercharging, b) 100 mM ammonium acetate (standard native MS solution), and c) 20 mM triethylammonium acetate, 80 mM ammonium acetate for charge-reducing native solutions. Asterisks denote apo-homodimers containing two β-subunits.

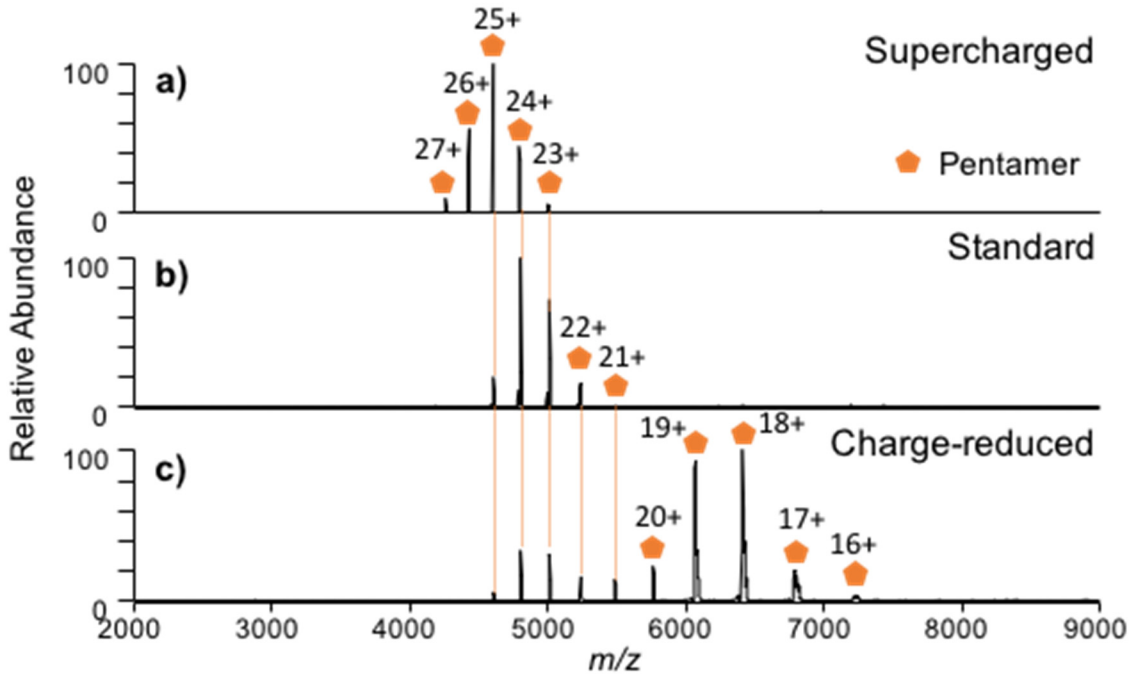

Figure S4. ESI-MS of C-reactive protein in a) 20 mM m-NBA, 80 mM ammonium acetate solution for supercharging, b) 100 mM ammonium acetate (standard native MS solution), and c) 20 mM triethylammonium acetate, 80 mM ammonium acetate for charge-reducing native solutions.

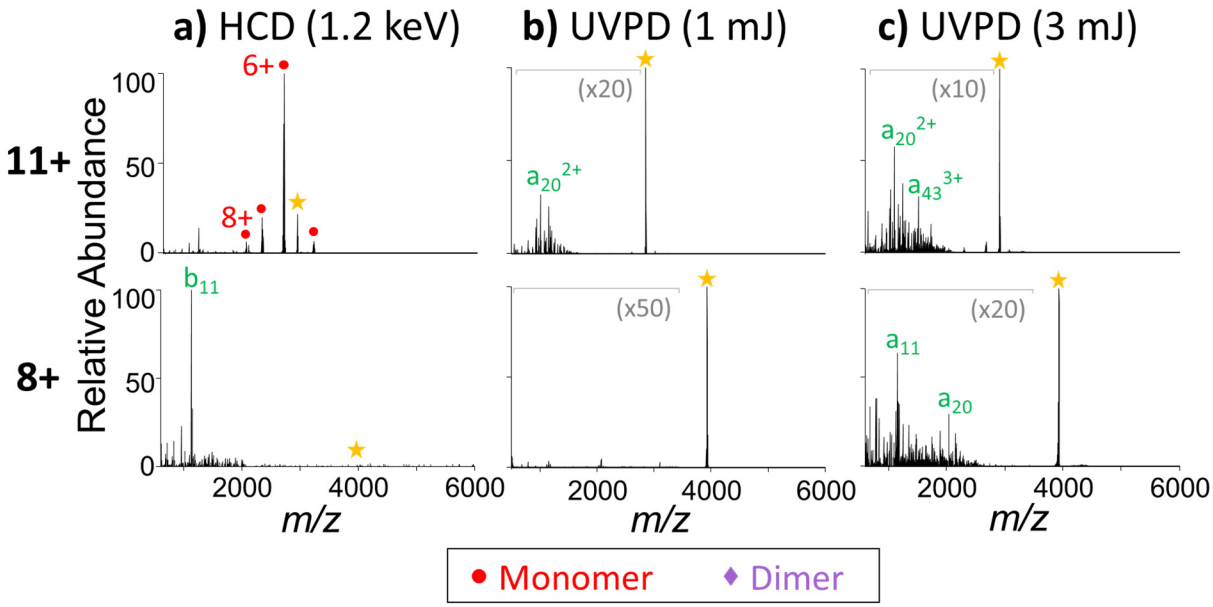

Figure S5. MS/MS spectra of 11+ (top) and 8+ SOD (bottom) using a) a lab frame collision energy of 1.2 keV for HCD, b) 1 mJ UVPD (1 pulse), and c) 3 mJ UVPD (1 pulse).

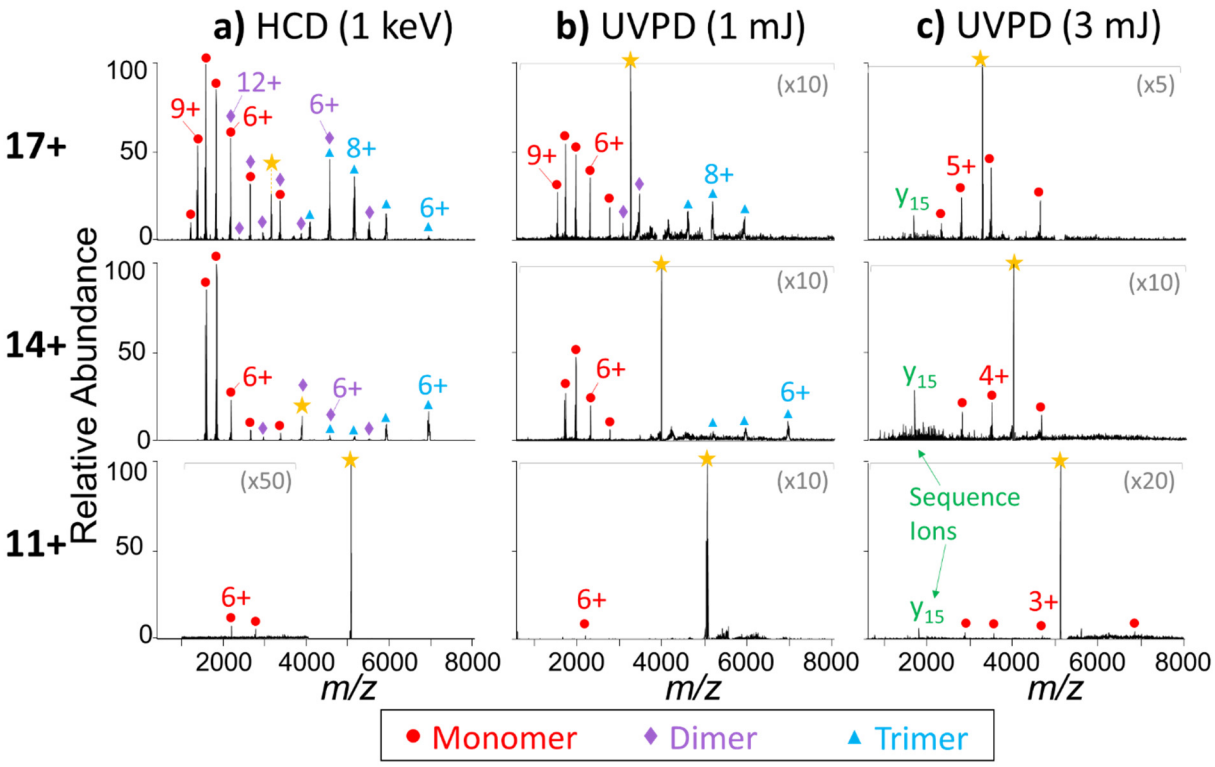

Figure S6. MS/MS spectra of transthyretin in 17+ (top) and 11+ (bottom) charge states using a) a lab frame collision energy of 1 keV for HCD, b) 1 mJ UVPD (1 pulse), and c) 3 mJ UVPD (1 pulse). The precursor ion is labelled with a star.

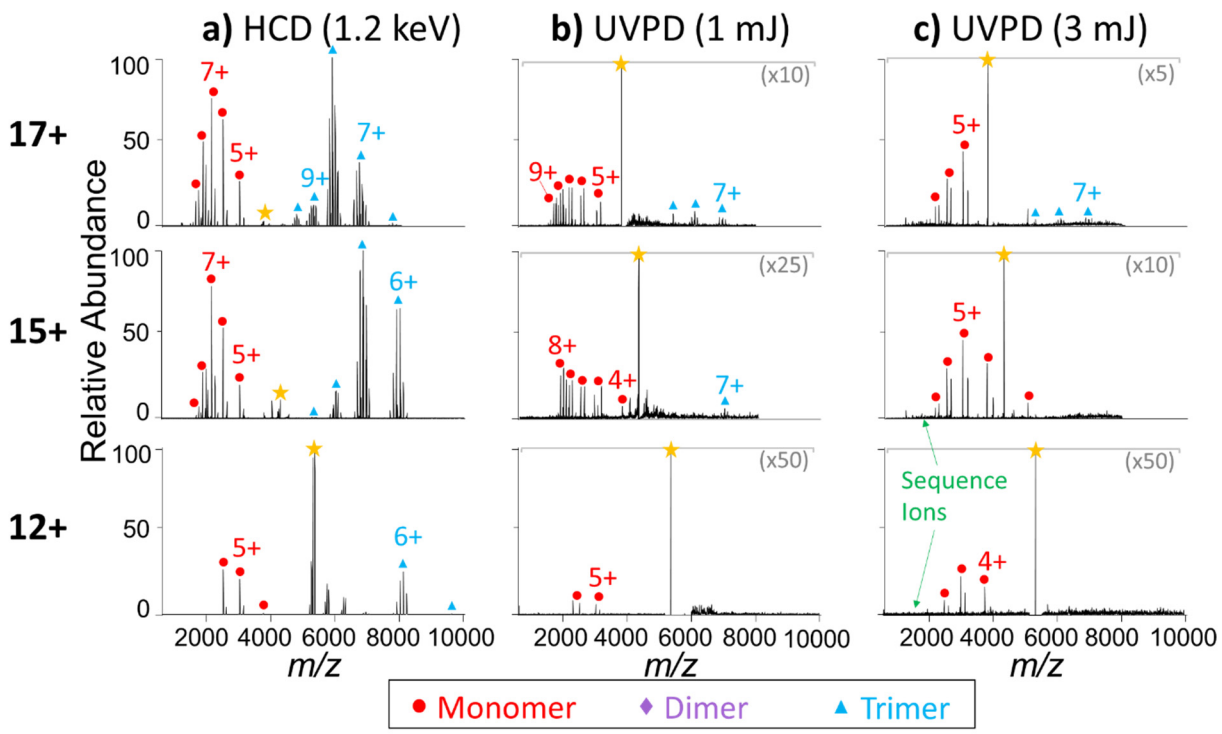

Figure S7. MS/MS spectra of hemoglobin in 17+ (top) and 12+ (bottom) charge states using a) a lab frame collision energy of 1 keV for HCD, b) 1 mJ UVPD (1 pulse), and c) 3 mJ UVPD (1 pulse). The precursor ion is labelled with a star. No dimeric products were observed.

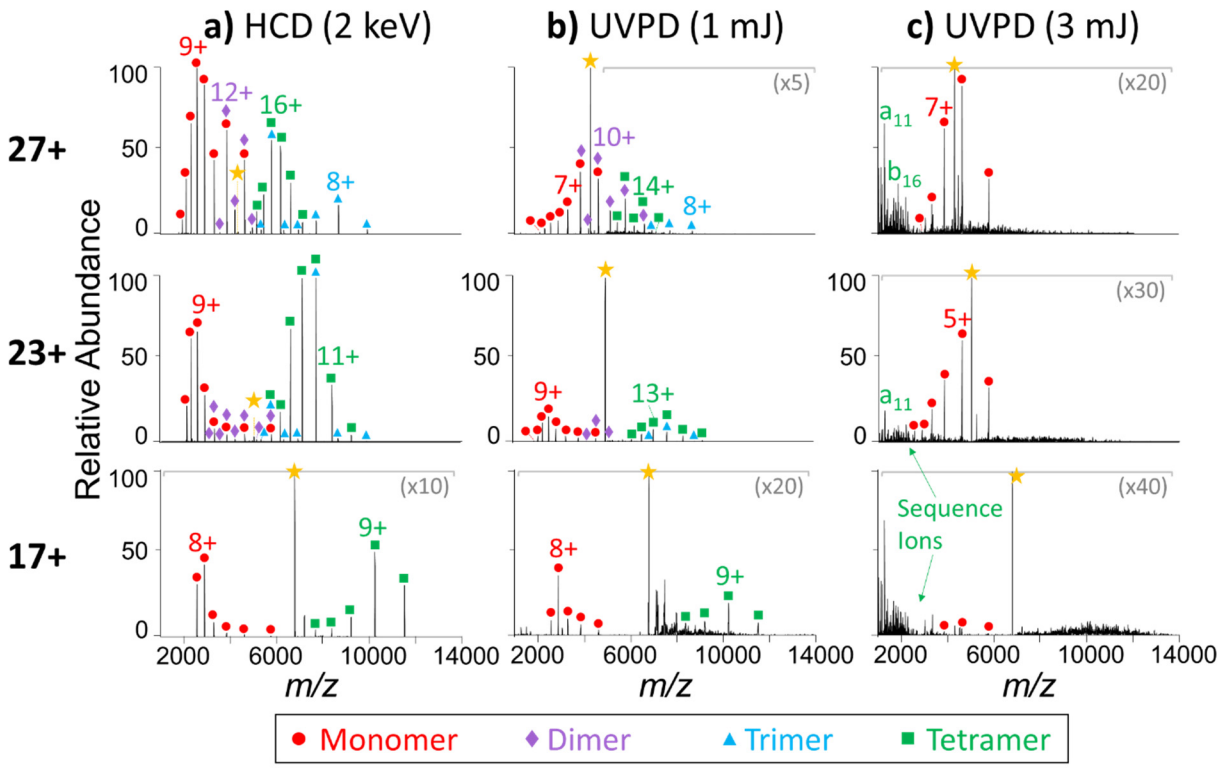

Figure S8. MS/MS spectra of C-reactive protein in 27+ (top) and 17+ (bottom) charge states using a) a lab frame collision energy of 1 keV for HCD, b) 1 mJ UVPD (1 pulse), and c) 3 mJ UVPD (1 pulse). The precursor ion is labelled with a star.

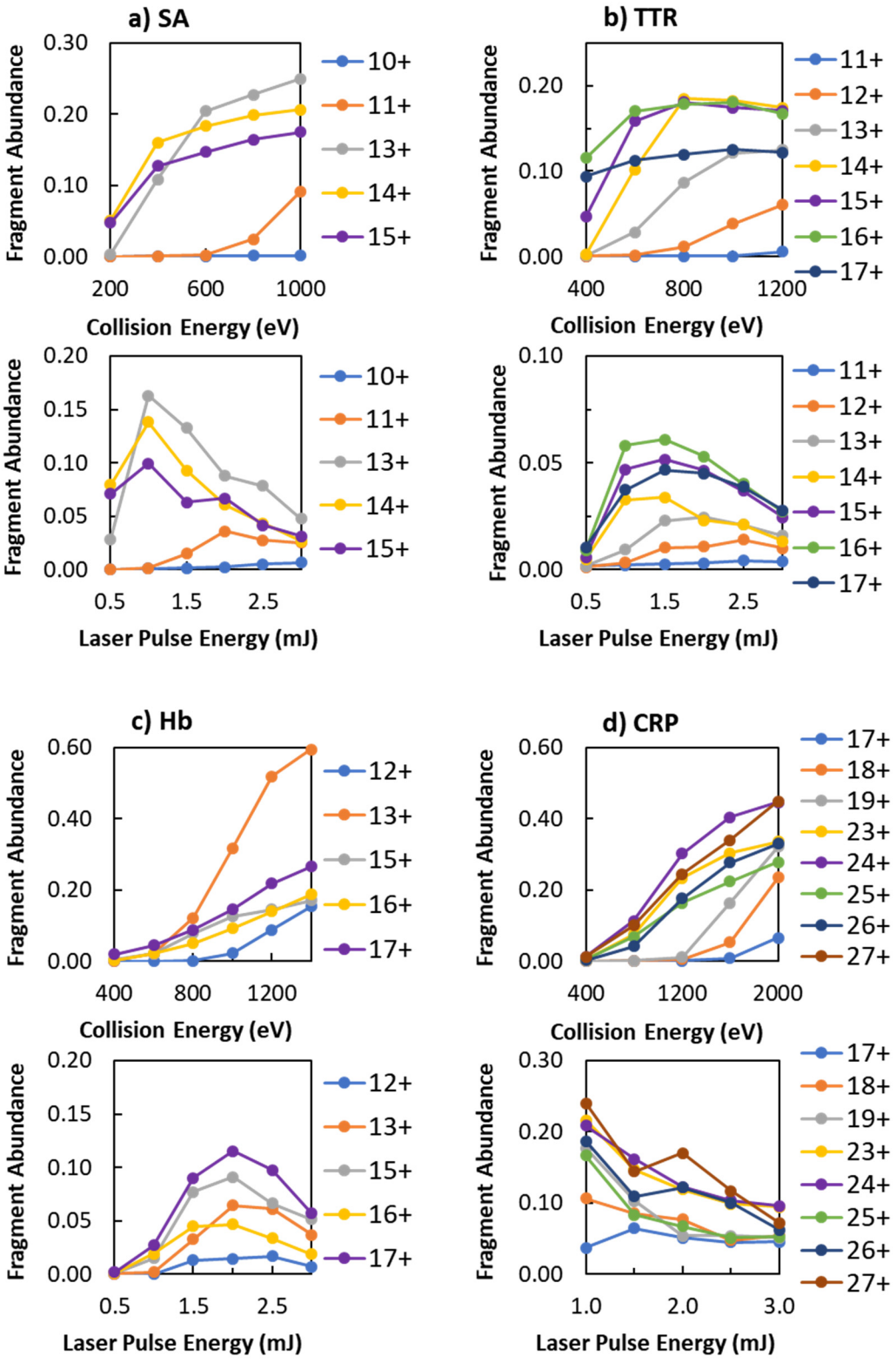

Figure S9. Fractional abundance of product ions normalized to the total ion current of each HCD or UVPD spectrum from selected precursors, as illustrated for a) 10+ to 15+ streptavidin, b) 11+ to 17+ transthyretin, c) 12+ to 17+ hemoglobin, and e) 17+ to 19+ and 23+ to 27+ CRP.

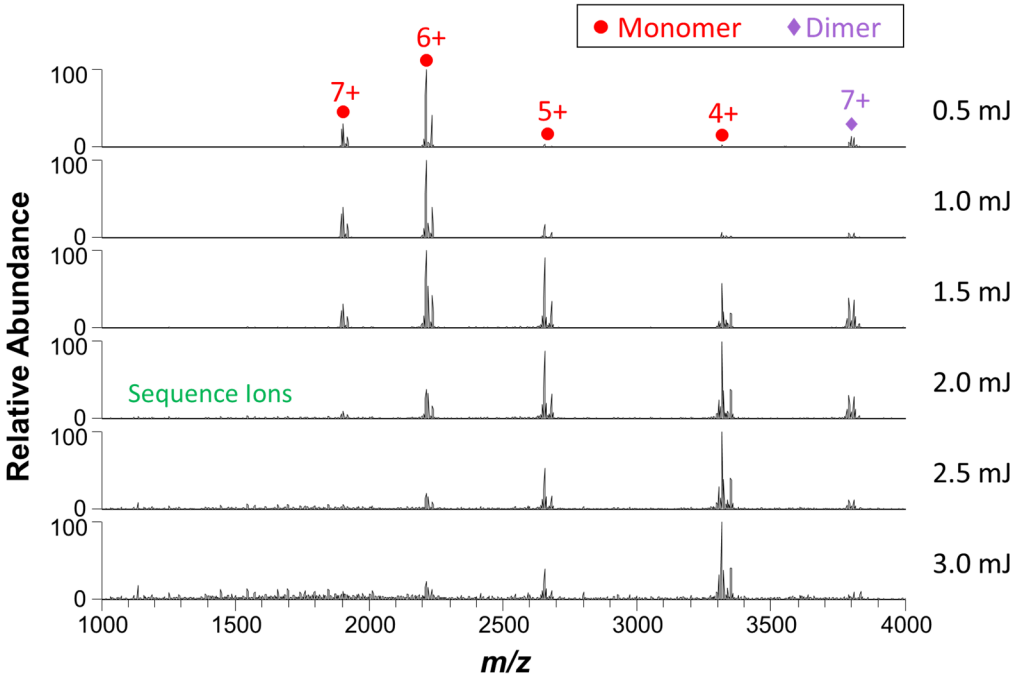

Figure S10. Truncated *m/z* range of UVPD mass spectra of 13+ streptavidin from standard native conditions activated with a single laser pulse with energy from 0.5 to 3.0 mJ. A shift to lower monomer charge state (higher *m/z*) is observed with increasing pulse energy.

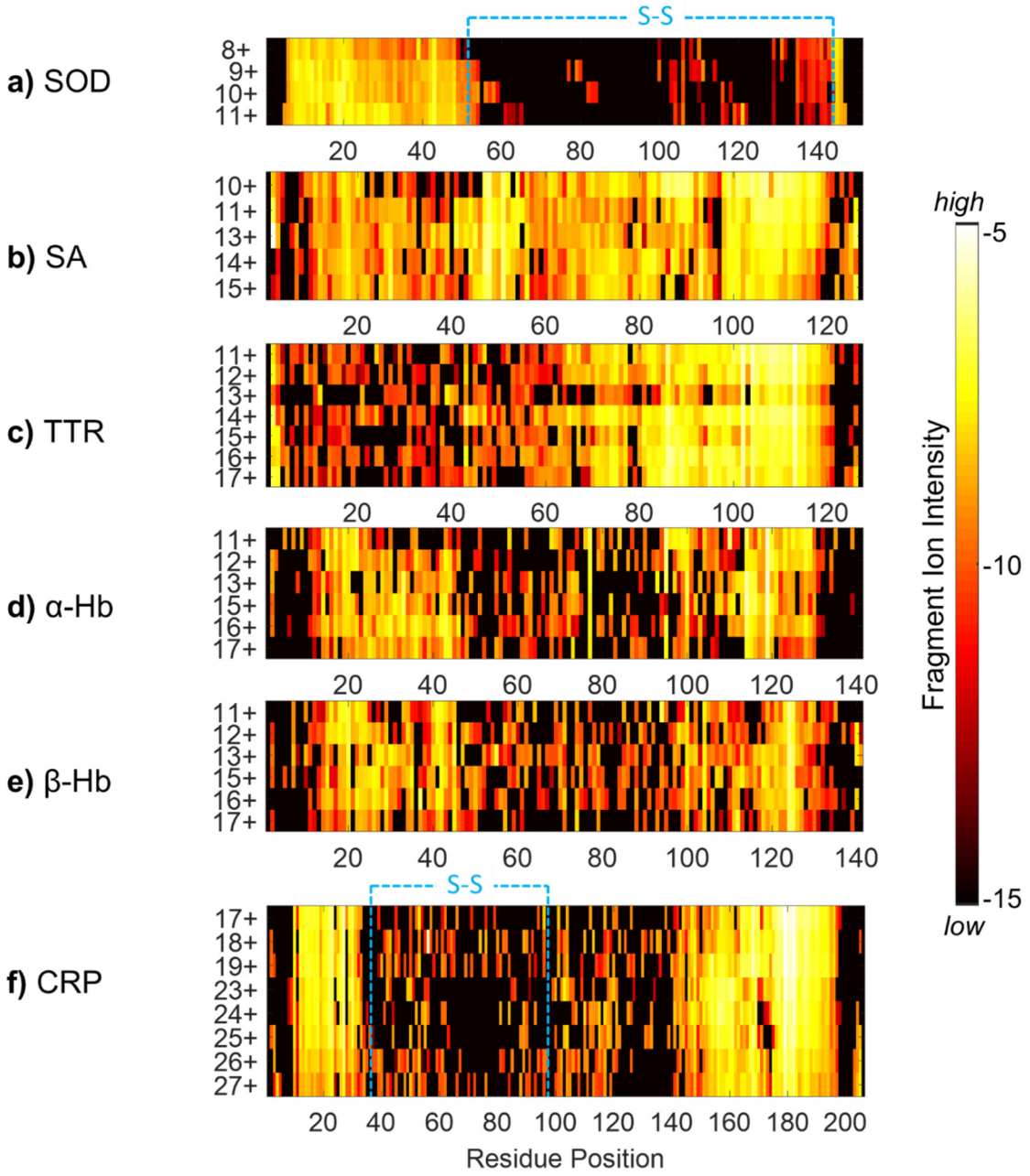

Figure S11. Location and relative abundance of sequence ions generated from 3 mJ UVPD of all of the charge states generated from supercharging, standard native, and charge-reducing solutions for a) superoxide dismutase, b) streptavidin, c) transthyretin, d) α-hemoglobin, e) β-hemoglobin, and f) C-reactive protein. The abundances of fragment ions that originate from cleavages at each backbone position are mapped from the N-terminus to the C-terminus across the entire protein sequence. The gradient scale shows the natural log of the fractional abundances of fragment ions with yellow representing the greatest abundance and black representing the lowest/no abundance.

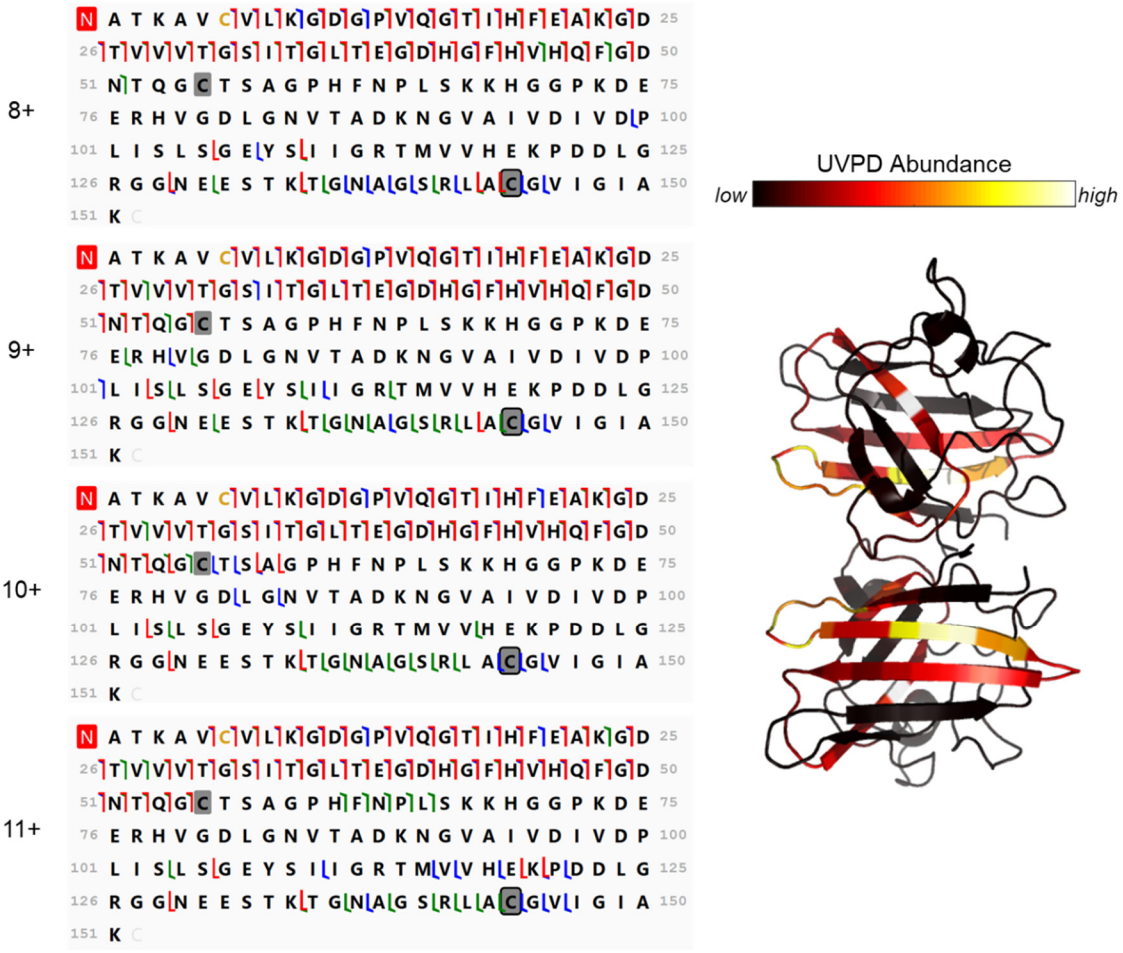

Figure S12. Fragment maps obtained using ProSight Lite for each charge state of SOD from 3 mJ UVPD (1 pulse). The red box on the N-terminus reflects the additional mass accounting for an acetylation modification. The gray boxes on Cys55 and Cys144 reflect the loss of one hydrogen each to account for the disulfide bond. Backbone cleavage markers are shown as colored flags: a,x: green; b,y: blue; c,z: red. On the right is the crystal structure of SOD (pdb 1cb4) colored to reflect the average normalized abundances of the backbone cleavages that yield the sequence ions on each fragment map.

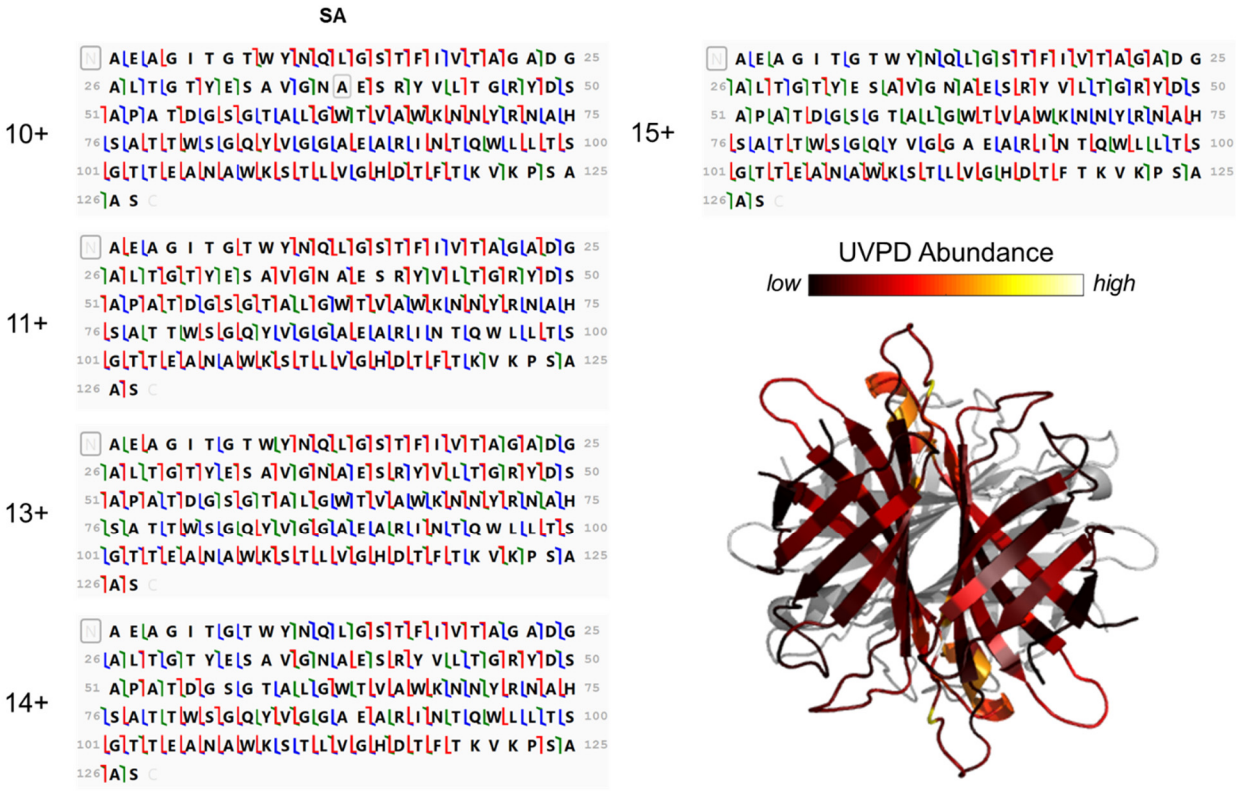

Figure S13. Fragment maps obtained using ProSight Lite for each charge state of SA from 3 mJ UVPD (1 pulse). Backbone cleavage markers are shown as colored flags: a,x: green; b,y: blue; c,z: red. On the right is the crystal structure of SA (pdb 1swe) colored to reflect the average normalized abundances of the backbone cleavages that yield the sequence ions on each fragment map.

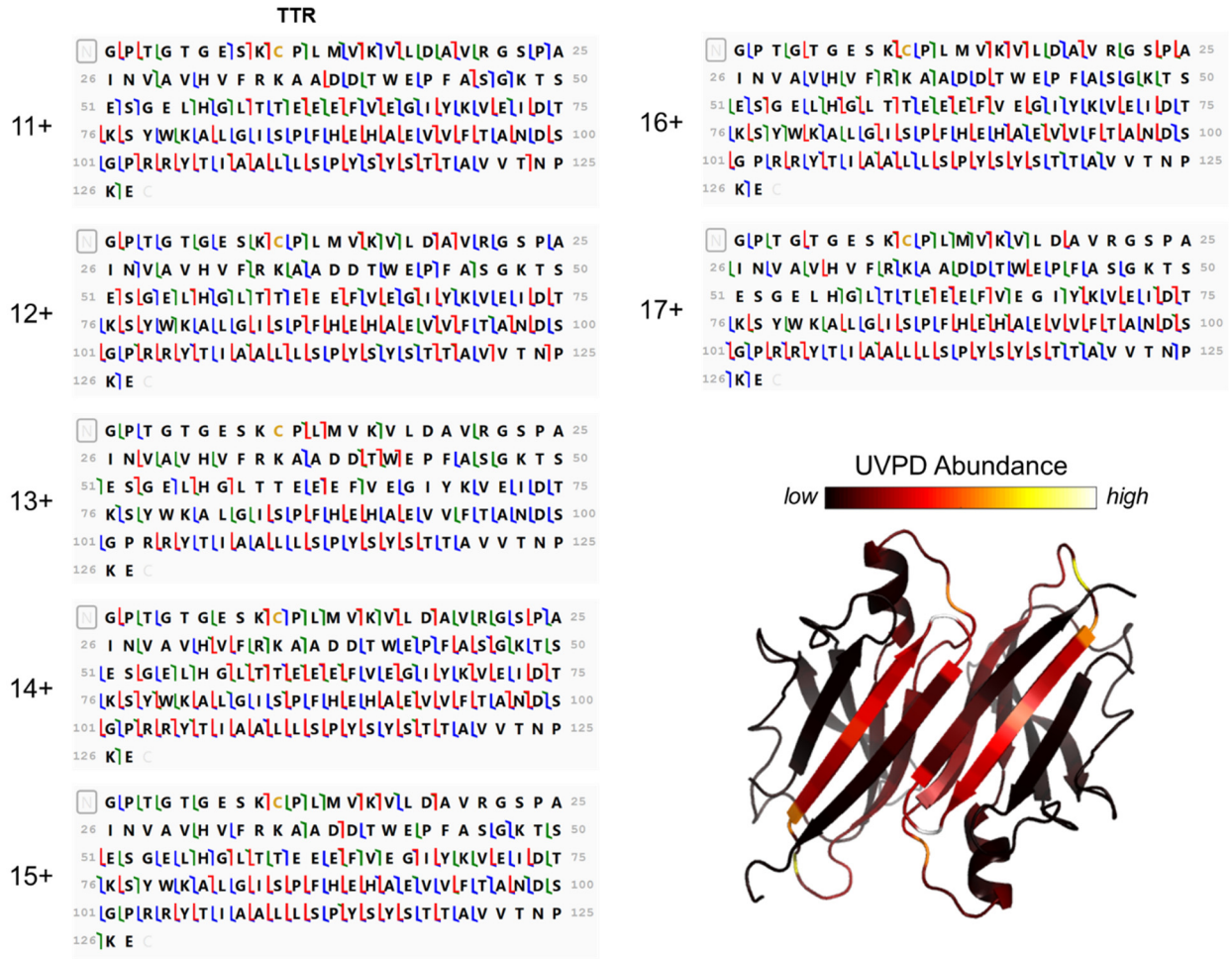

Figure S14. Fragment maps obtained using ProSight Lite for each charge state of TTR from 3 mJ UVPD (1 pulse). Backbone cleavage markers are shown as colored flags: a,x: green; b,y: blue; c,z: red. On the right is the crystal structure of TTR (pdb 2rox) colored to reflect the average normalized abundances of the backbone cleavages that yield the sequence ions on each fragment map.

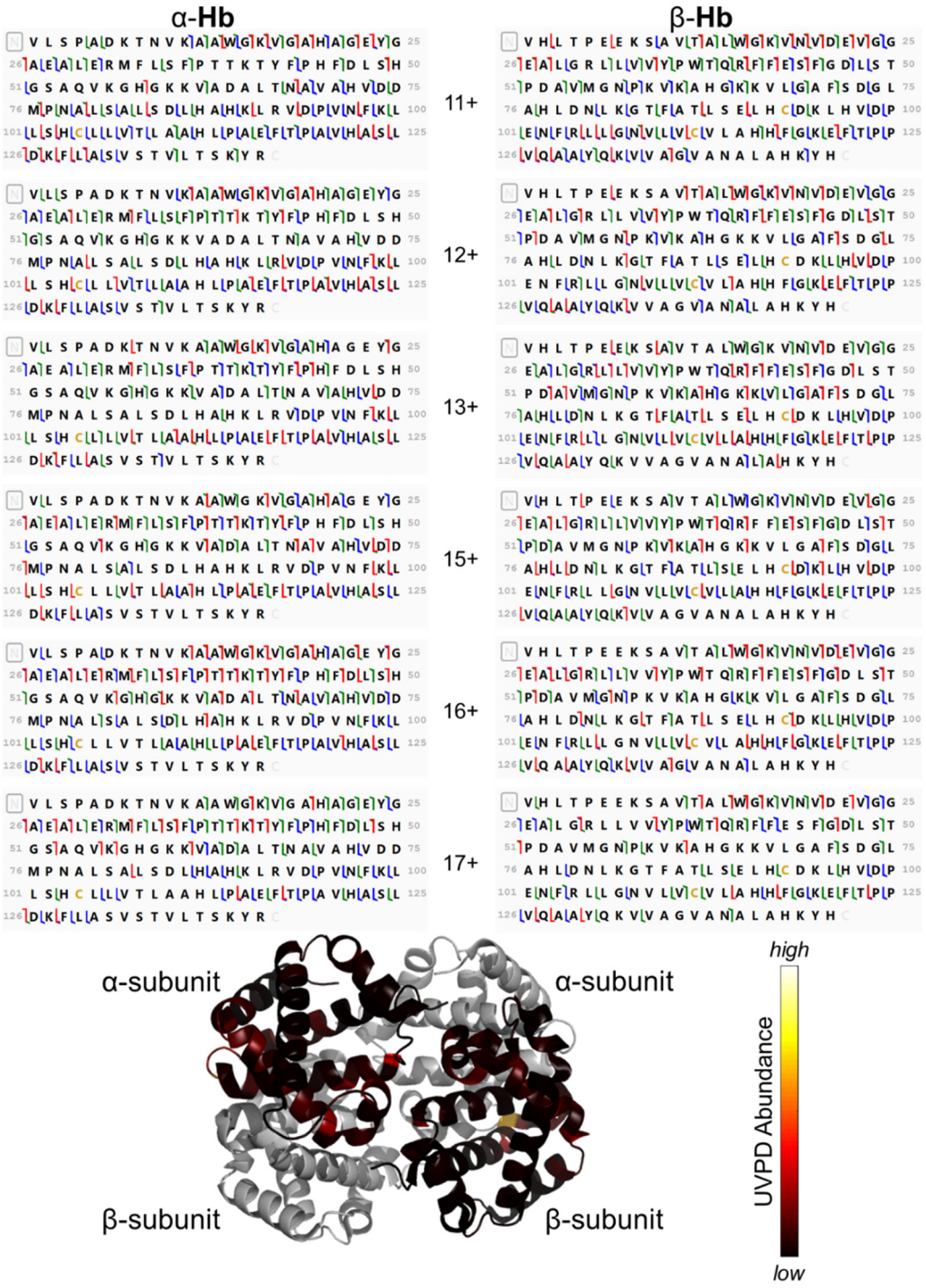

Figure S15. Fragment maps obtained using ProSight Lite for each charge state of Hb from 3 mJ UVPD (1 pulse) for the alpha subunit (left) and beta subunit (right). Backbone cleavage markers are shown as colored flags: a,x: green; b,y: blue; c,z: red. On the bottom is the crystal structure of Hb (pdb 1qzx) colored to reflect the average normalized abundances of the backbone cleavages that yield the sequence ions on each fragment map.

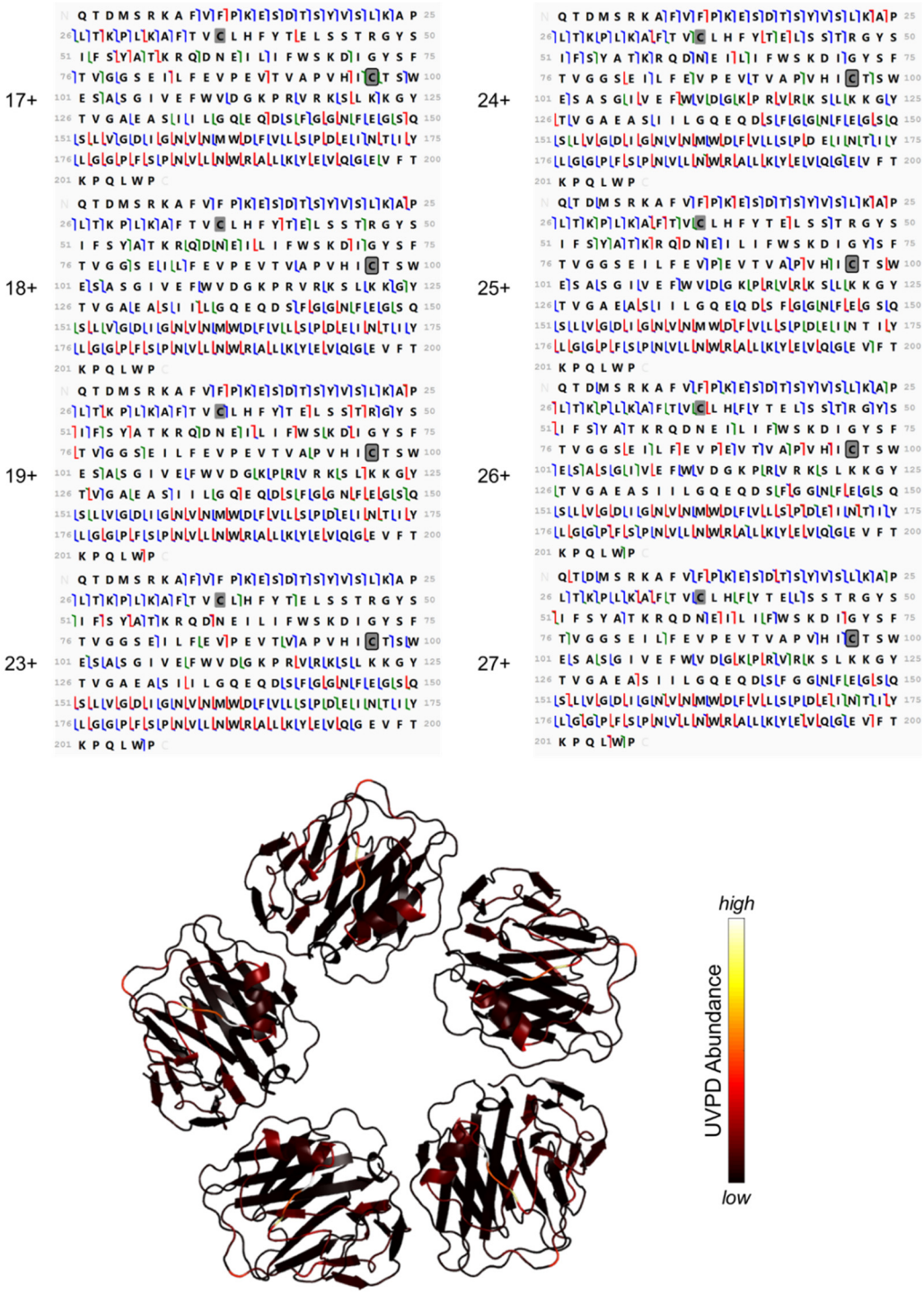

Figure S16. Fragment maps obtained using ProSight Lite for each charge state of CRP from 3 mJ UVPD (1 pulse). The gray boxes on Cys36 and Cys97 reflect the loss of one hydrogen each to account for the disulfide bond. Backbone cleavage markers are shown as colored flags: a,x: green; b,y: blue; c,z: red. On the bottom is the crystal structure of CRP (pdb 1b09) colored to reflect the average normalized abundances of the backbone cleavages that yield the sequence ions on each fragment map.

.

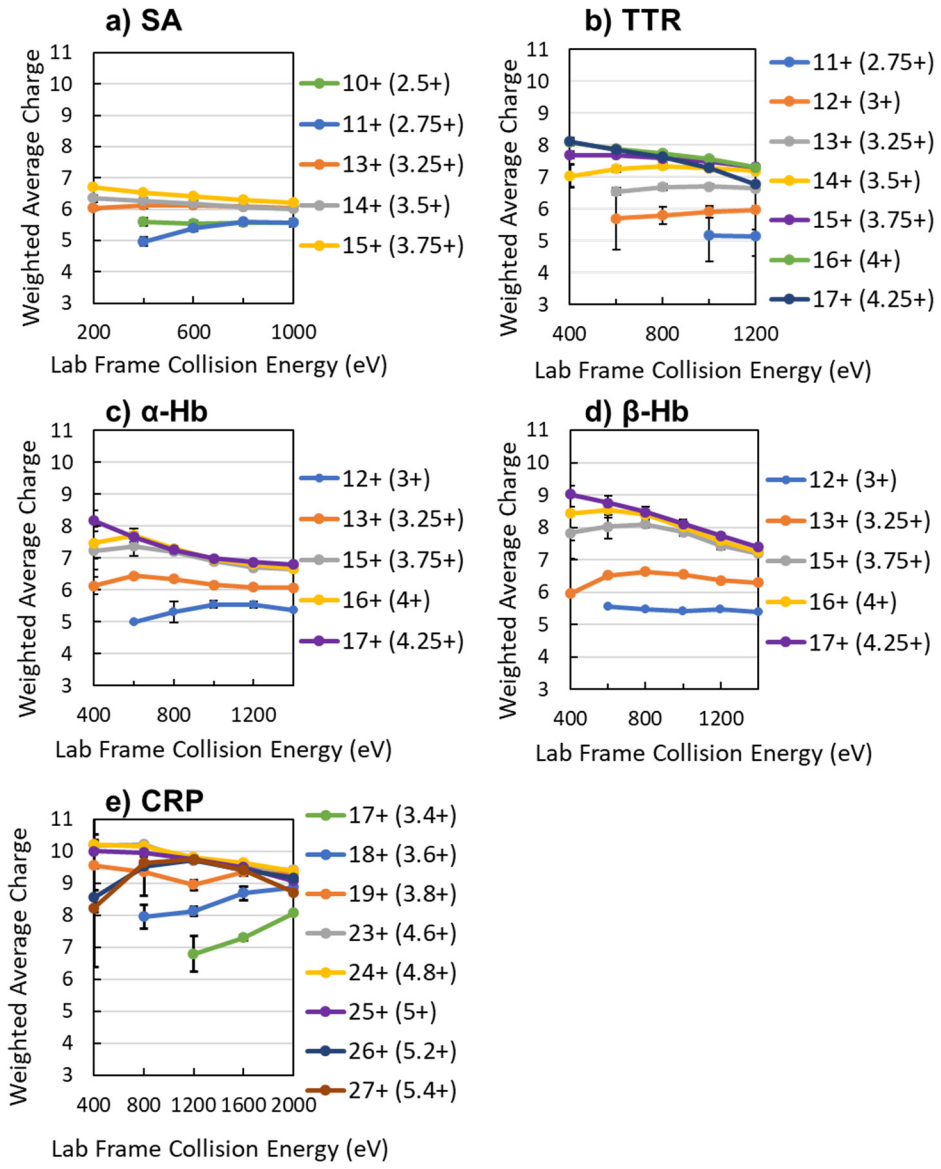

Figure S17. Weighted average charge of ejected monomers using varying lab frame collision energies for HCD of the precursors of a) 10+ to 15+ streptavidin, b) 11+ to 17+ transthyretin, c,d) 12+ to 17+ hemoglobin, and e) 17+ to 19+ and 23+ to 27+ CRP. Ejected monomers of Hb are shown separately as c) α-subunits and d) β-subunits. Error bars indicate the standard deviation of replicate data. Values in parentheses next to each precursor charge indicate the theoretical charge state of each monomer following charge-symmetric partitioning.

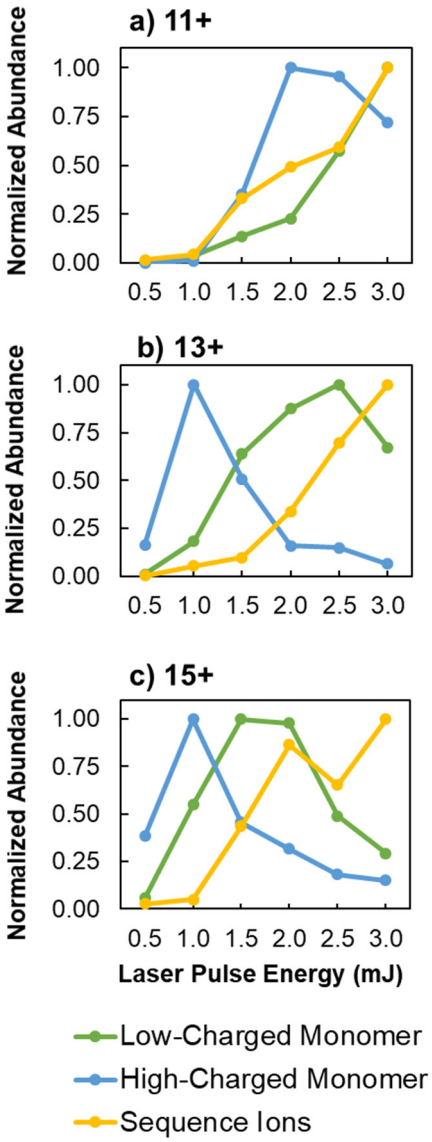

Figure S18. Energy variable fragmentation graphs showing the abundance of low-charged monomers (3+, 4+), high-charged monomers (5+, 6+), and sequence ions from the a) 11+, b) 13+, and c) 15+ precursors of SA using varying laser pulse energies for UVPD.

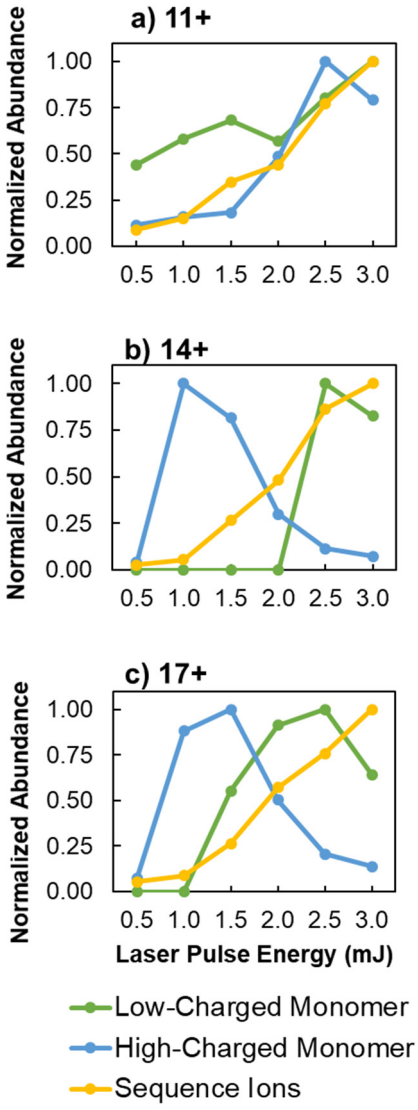

Figure S19. Energy variable fragmentation graphs showing the abundance of low-charged monomers (3+, 4+), high-charged monomers (5+, 7+), and sequence ions from the a) 11+, b) 14+, and c) 17+ precursors of TTR using varying laser pulse energies for UVPD.

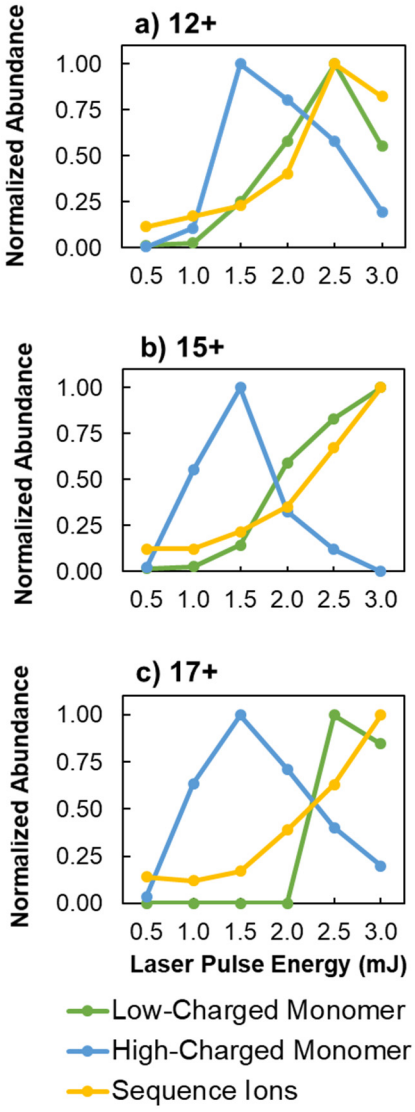

Figure S20. Energy variable fragmentation graphs showing the abundance of low-charged monomers (4+), high-charged monomers (6+, 8+), and sequence ions from the a) 12+, b) 15+, and c) 17+ precursors of α-Hb using varying laser pulse energies for UVPD.

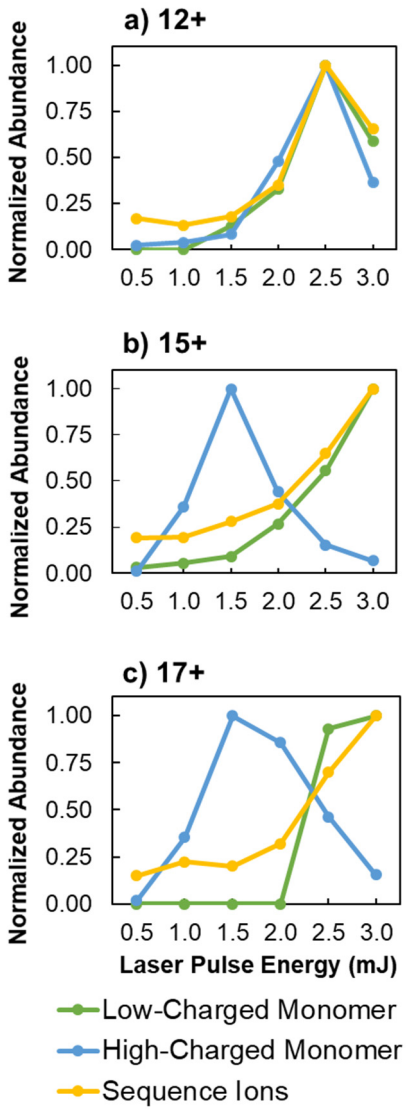

Figure S21. Energy variable fragmentation graphs showing the abundance of low-charged monomers (4+), high-charged monomers (6+, 8+), and sequence ions from the a) 12+, b) 15+, and c) 17+ precursors of β-Hb using varying laser pulse energies for UVPD.

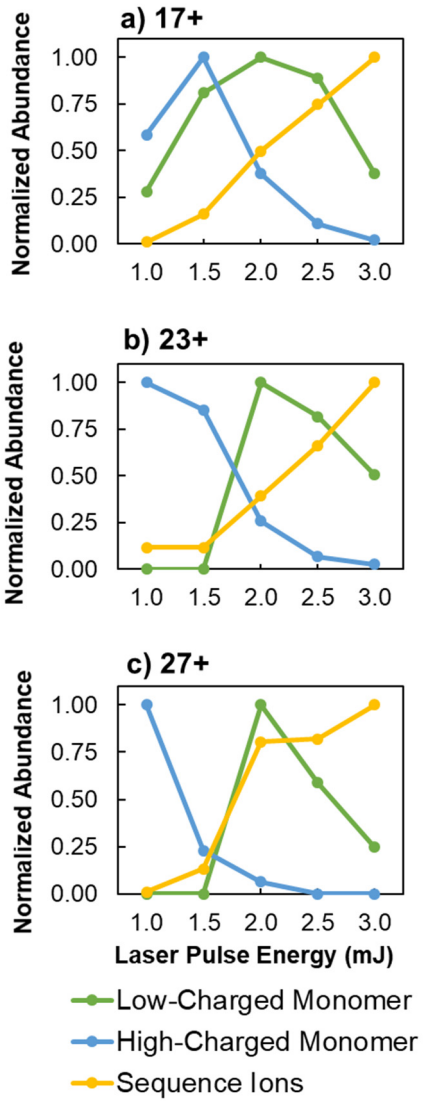

Figure S22. Energy variable fragmentation graphs showing the abundance of low-charged monomers (5+), high-charged monomers (8+, 9+), and sequence ions from the a) 17+, b) 23+, and c) 27+ precursors of CRP using varying laser pulse energies for UVPD.

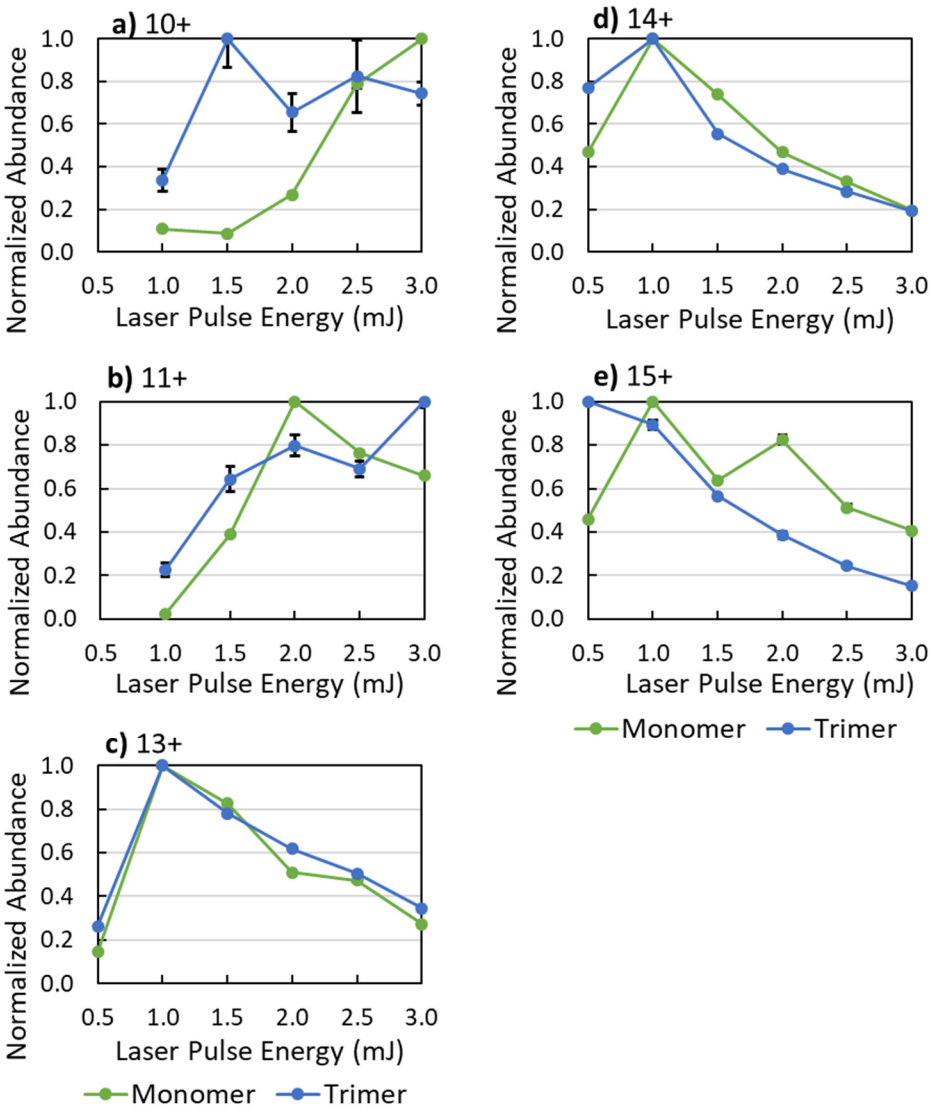

Figure S23. Energy variable fragmentation graphs showing the summed abundance of monomers and trimers from charge reduced (a, b), standard (c, d), and supercharged streptavidin (e) upon UVPD.

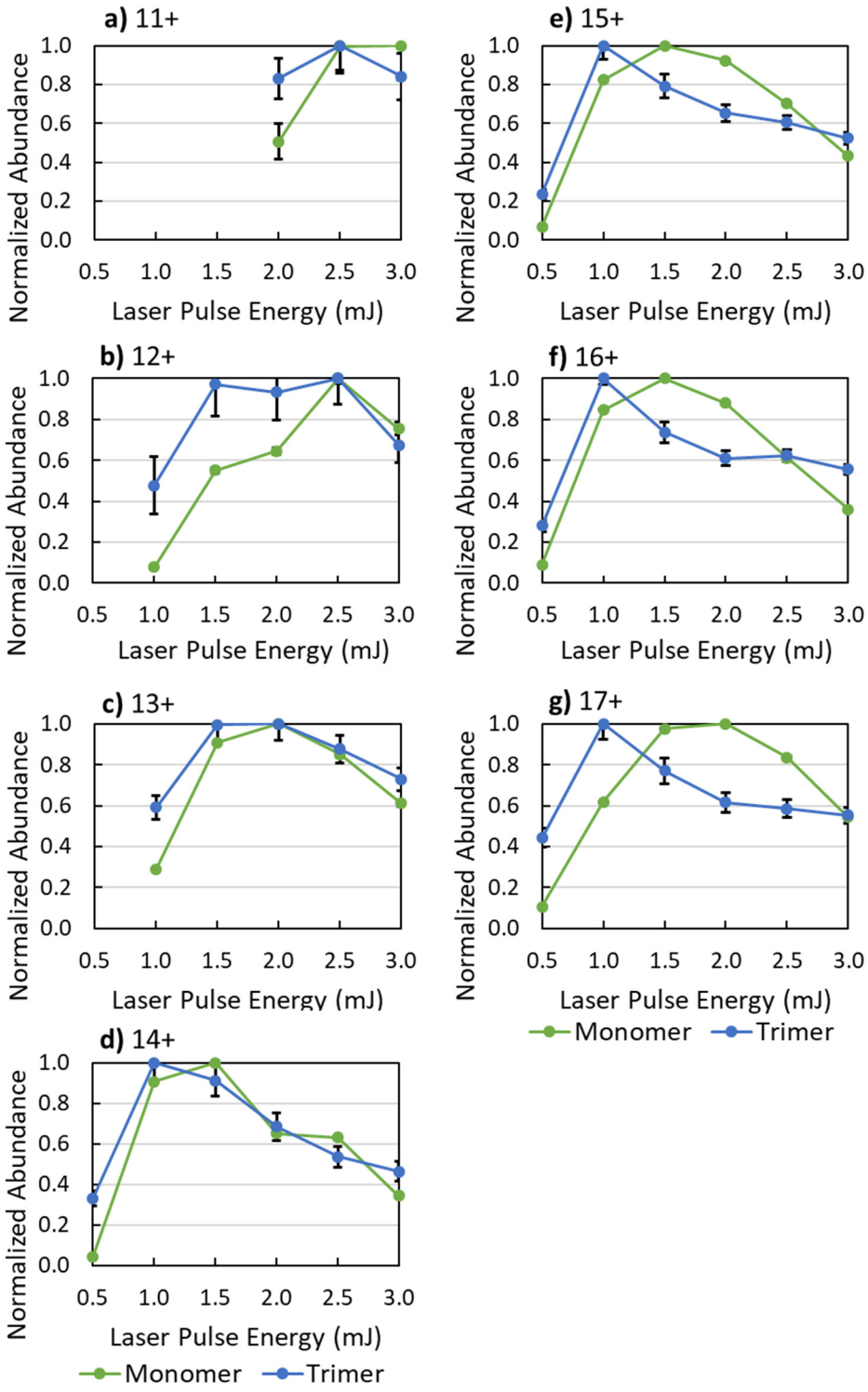

Figure S24. Energy variable fragmentation graphs showing the summed abundance of monomers and trimers from charge reduced (a, b), standard (c, d, e), and supercharged transthyretin (f, g) upon UVPD.

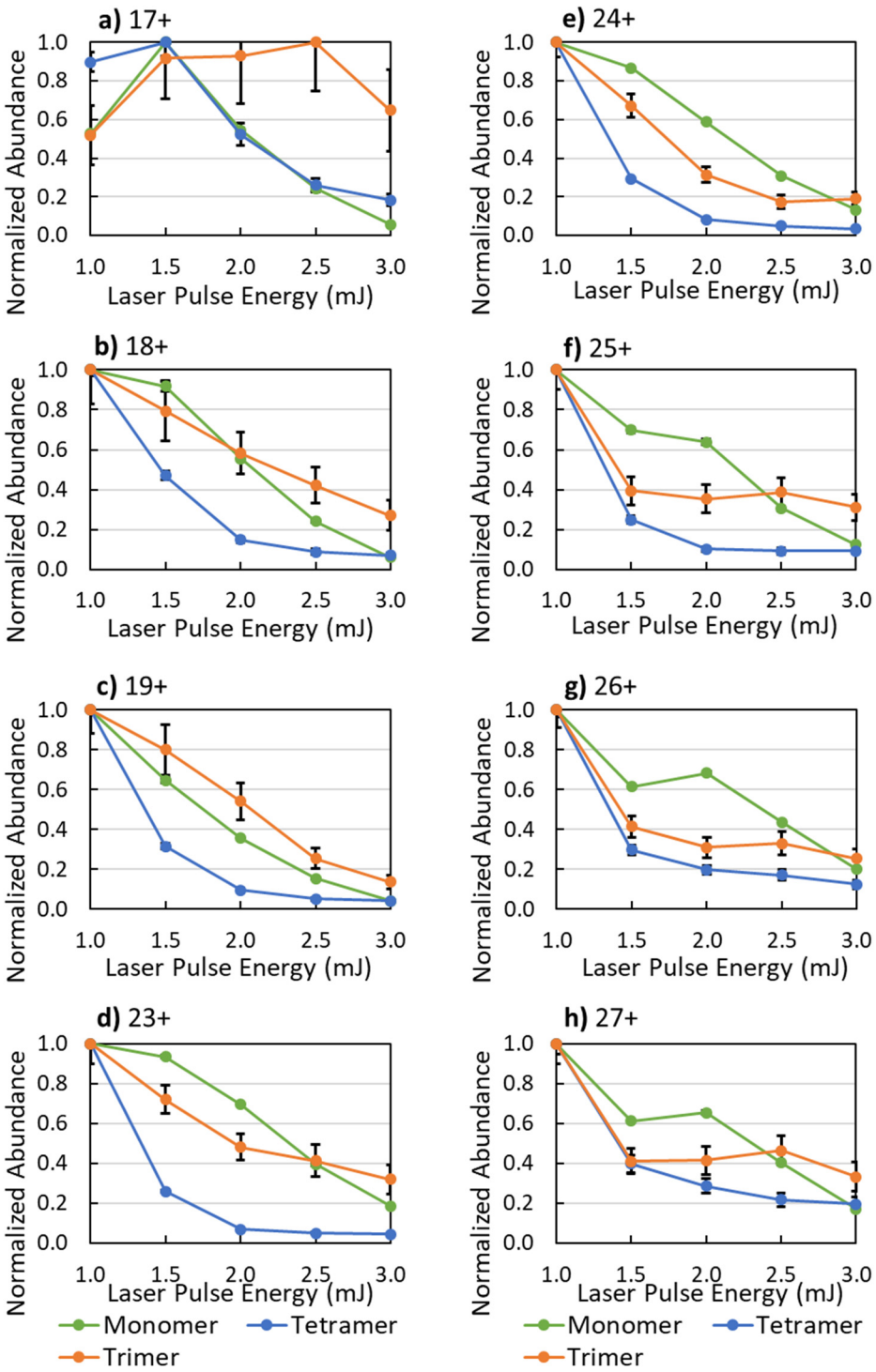

Figure S25. Energy variable fragmentation graphs showing the summed abundance of monomers, trimers, and tetramers from charge reduced (a, b, c), standard (d, e, f), and supercharged C-reactive protein (g, h) upon UVPD. Charge states of tetramers and trimers that overlap with other subcomplexes were not included (e.g. 12+ trimer, 16+ tetramer).